Supporting Information

Zhang et al. 10.1073/pnas.1113220108

SI Materials and Methods

Antibodies and Reagents. A rabbit polyclonal antibody against mouse Bbs3 peptide DKTARYWRIK was obtained from Open Biosystems. A rabbit polyclonal antibody against human Bardet-Biedl syndrome-3 (BBS3) was a gift from Max Nachury (Stanford University, Palo Alto, CA). All antibodies were affinity-purified and verified in knockout mice or by RNAi. Monoclonal anti–β-tubulin, polyclonal anti–β-actin, monoclonal antiacetylated tubulin, monoclonal anti–γ-tubulin, rabbit polyclonal anti-BBS8, and BBS9 were purchased from Sigma. Goat anti-BBS2 (C-16), rabbit anti-ACIII, and goat antimelanin concentrating hormone receptor 1 (anti-MCHR1) antibodies were purchased from Santa Cruz Biotechnology. Alexa 488 conjugated cholera toxin and Alexa 568 conjugated human transferring receptor were purchased from Invitrogen. Adenoviruses expressing Flag-BBS1, BBS2, or BBS4 were gifts from Michael Welsh (University of Iowa, Iowa City, IA). Smartpool RNAi against human BBS2, BBS3, BBS8, and BBS9 were from Dharmacon. Cell culture, transfection, and immunofluorescence microscopy 293T cells were cultured in DMEM high glucose with 10% FBS, hTERT-immortalized retinal pigment epithelial (RPE1) cells were cultured in DMEM/F-12 medium with 10% serum. All tansfections were done using lipofectamine 2000 (Invitrogen). For RNAi transfection, a final concentration of 100 nM RNAi was used. For immunofluorescence, cells were fixed in cold methanol for 5 min at −20 °C and were washed three times with PBS and blocked with blocking buffer (1% BSA in PBS). Primary antibodies were diluted in blocking buffer and incubated at room temperature for 1 h. Cells were washed three times with PBS, blocked with blocking buffer, then incubated with Alexa 488 or Alexa 568-labeled secondary antibodies (Invitrogen). Nuclei were stained with DAPI (Sigma). Images were taken with an Olympus BX-41 microscope with a CCD camera.

Differential Ultracentrifugation and Sucrose Gradient Fractionation. Tissues were disrupted by TISSUEMISER (Fisher Scientific) in the fractionation buffer (10 mM Hepes, pH 7.4, 3 mM $MgCl_2$, 1 mM EDTA, 5% sucrose) and sonicated. The lysates were centrifuged twice at 600 × *g* for 20 min. The supernatants were centrifuged at 128,000 × *g* for 1 h. The pellet was quickly washed once with fraction buffer and resuspended in fractionation buffer by sonication. The suspension was loaded onto a 20–60% sucrose gradient. Membrane fractions were loaded onto the gradient and centrifuged for 14 h using a TH-660 rotor Thermo Scientific. Three hundred microliter fractions were taken from the top and diluted with 10× volume of fractionation buffer and were pelleted by ultracentrifugation at 200,000 × *g* for 30 min. The pellets were washed once with fraction buffer and dissolved in SDS/PAGE sample buffer.

Histological Analysis of *Bbs3*$^{-/-}$ Mice. H&E staining of eyes and testes from 2- to 8.5-mo-old *Bbs3*$^{-/-}$ (n = 3) and age-matched controls (n = 3) was carried out as previously described (1) Photographs were taken with an Olympus BX-41 microscope with a SPOT-RT digital camera. Sixty- to 100-mm coronal brain sections of 8.5-mo-old *Bbs3*$^{-/-}$ animals (n = 3) and age-matched controls (n = 3) were stained with Neutral red and photographed with an Olympus SZX12 stereomicroscope as previously described (2).

H&E staining was also performed for *Bbs3*$^{-/-}$ mice and age-matched controls at one week of age (P5, n = 3). Ten- to 12-μm sections were taken and analyzed for ventricular dilation. These sections were processed and imaged as above.

Body Weight Studies. Food intake of individually housed *Bbs3*$^{-/-}$ animals was compared with WT control animals ranging in age from 4 to 28 wk using an average of six animals per group. Body weight was recorded weekly beginning at weaning.

Generation of *Bbs3* Knockout Mice. PCR was used to amplify 5′ and 3′ regions of the *Bbs3* gene from 129/SvJ genomic DNA and cloned into the targeting vector pOSDUPDEL (a gift from O. Smithies, University of North Carolina, Chapel Hill, NC). The vector was linearized and electroporated into R1 ES cells (129 × 1/SvJ3 129S1/Sv). G418 and ganciclovir-resistant clones were screened by long range PCR to identify correctly targeted ES cell lines. Two independent ES cell lines were used to produce chimeras. Chimeric animals were used to generate *Bbs3* heterozygous mice on a mixed genetic background by mating with C57BL/6J mice. Heterozygous mice were intercrossed, and the progeny were genotyped by PCR. All studies adhered to the guidelines established for the care and use of experimental animals and were approved by the Animal Care and Use Committee of the University of Iowa.

Quantitative RT-PCR. RNA was isolated from WT and *Bbs3*$^{-/-}$ MEF cells using TRIzol reagent (Invitrogen) following the manufacturer's instructions. One microgram of total RNA was used for cDNA synthesis with random primers and SuperScript II reverse transcriptase (Invitrogen). Quantitative PCR was performed with SYBR Green Supermix (Bio-Rad) and Mx3000P qPCR System (Stratagene).

Generation of Mouse Embryonic Fibroblast Cells. WT and *Bbs3*$^{-/-}$ primary mouse embryonic fibroblasts (MEF) were generated from embryonic day 13.5 embryos and cultured in DMEM with 10% FBS and penicillin/streptomycin. To induce cilia formation, MEF cells were grown to 80–90% confluency and serum starved for 24 h; cells were treated with DMSO or 100 nM SAG (a Smoothened-binding Sonic hedgehog pathway agonist) for 16–20 h.

Scanning Electron Microscopy. Cultured brain ependymal cells from WT and *Bbs3*$^{-/-}$ mice were dehydrated in ethanol and dried by using a critical point drier. The samples were then mounted on an aluminum stub by using double-stick carbon tape, coated with gold/palladium by using a sputter coater, and then examined on a Philips XL 30 scanning electron microscope.

Ependymal Cell Culture and Ciliary Beating Frequency. Brains from *Bbs3*$^{-/-}$ and WT mice were taken at P0 and dissected to procure cells in the lateral and third ventricles. These cells were grown separately in DMEM with 10% FBS and allowed to differentiate to multiple ciliated ependymal cells on transparent transwell inserts in 12-well plates. Cultured ependymal cells were transferred to a 37 °C temperature-controlled stage and imaged on a Zeiss LSM 510 META NLO. Ciliated cells were randomly selected and movies of ciliary beating frequency were then generated. Line scans of cilia movement were collected. Data were analyzed by using National Institutes of Health ImageJ software.

Immunoprecipitation. Differentially tagged human BBS genes were cotransfected into 293T cells. Forty-eight hours after transfection, the cells were lysed in lysis buffer (1× PBS, 1% Triton X-100, and protease inhibitor; Roche) and spun at 20,000 × *g* for 15 min at 4 °C. The supernatants were cleared by incubation with protein G beads (Pierce). Cleared lysates were incubated with antibodies against corresponding tags for 4 h. Protein G beads were then

added and incubated for another 4 h. The beads were washed four times with lysis buffer and the interactions were detected by Western blotting.

Western Blotting. *Bbs3* WT and mutant testes were disrupted by TISSUEMISER (Fisher Scientific) in lysis buffer (1× PBS, 1% Triton X-100, and protease inhibitor, Roche). The disrupted tissues were freeze-thawed three times. The lysates were then centrifuged at 20,000 × *g* for 15 min and the concentration of the supernatants was measured using the Bio-Rad Dc protein assay.

Immunoprecipitated proteins were separated by electrophoresis using 4–12% NuPAGE Bis-Tris gels (Invitrogen) followed by transfer to nitrocellulose membranes and were detected by SuperSignal Dura extended substrate (Pierce).

1. Mykytyn K, et al. (2004) Bardet-Biedl syndrome type 4 (BBS4)-null mice implicate Bbs4 in flagella formation but not global cilia assembly. *Proc Natl Acad Sci USA* 101: 8664–8669.

2. Davis RE, et al. (2007) A knockin mouse model of the Bardet-Biedl syndrome 1 M390R mutation has cilia defects, ventriculomegaly, retinopathy, and obesity. *Proc Natl Acad Sci USA* 104:19422–19427.

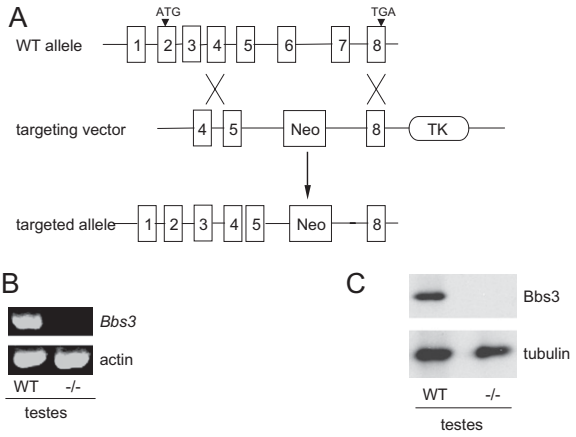

Fig. S1. Generation of *Bbs3* knockout mice. (*A*) Diagram of the Bbs3 targeting vector and the resulting recombination product. (*B*) RT-PCR analysis of *Bbs3* expression in testis total cellular RNA from WT and $Bbs3^{-/-}$ animals. (*C*) Western blot analysis of WT and $Bbs3^{-/-}$ testes confirms the absence of the 20-kDa Bbs3 protein.

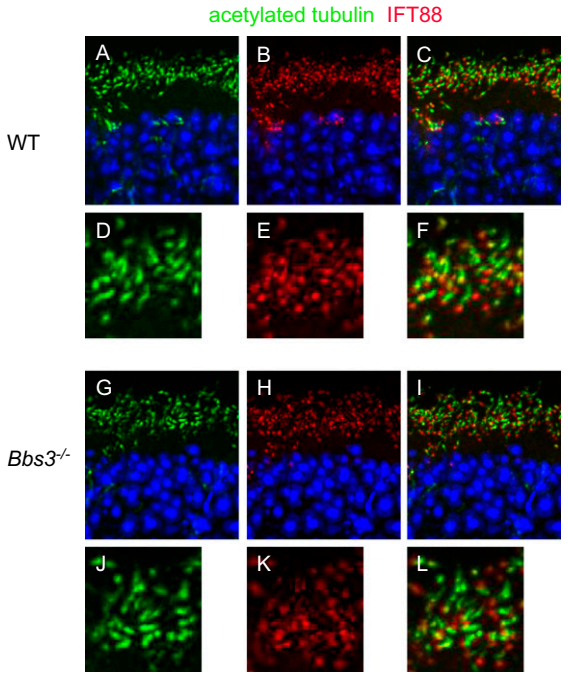

Fig. S2. BBS3 is not required for primary ciliogenesis. Shown are confocal images of frozen mouse eye tissue sections stained with antiacetylated α-tubulin (green) and IFT88 (red). (*A–F*) Immunofluoresence staining of WT mouse eyes. (*D–F*) The enlargement of *A* to *C*. (*G–L*) Immunofluoresence staining of $Bbs3^{-/-}$ mouse eyes. (*J–L*) Enlargement (3×) of *G* to *I*. Similar results are obtained for cultured kidney cells, kidney tissue sections, and pancreas tissue sections.

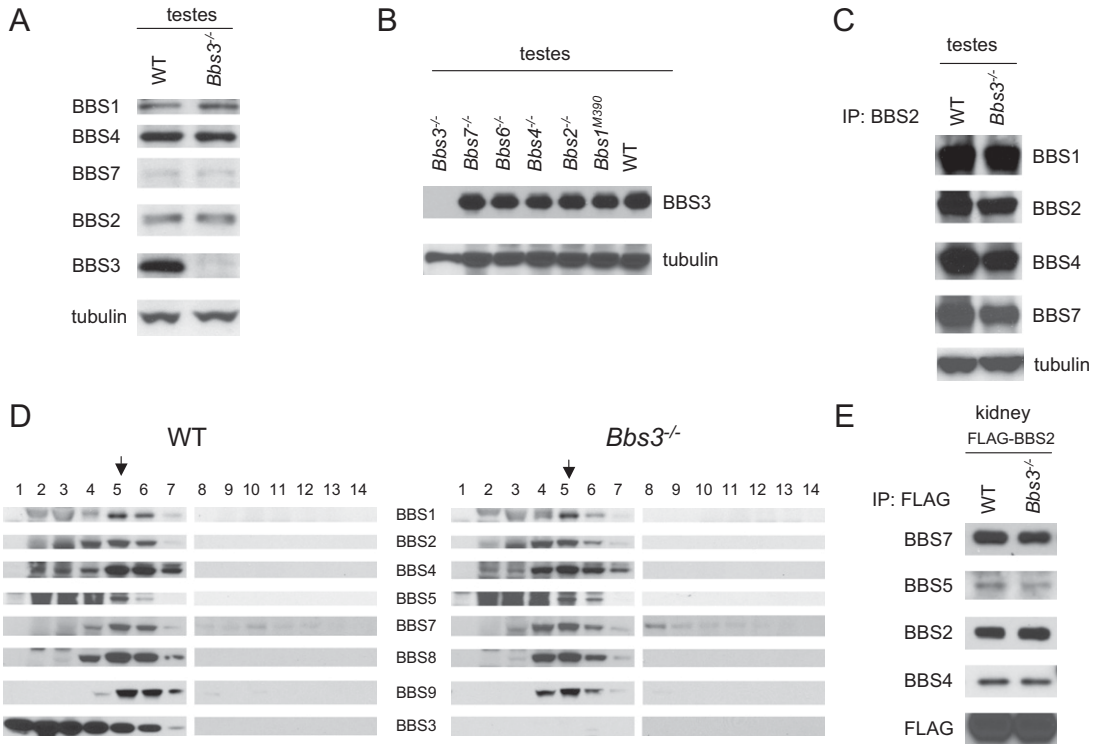

Fig. S3. BBS3 is not required for BBSome formation. (*A*) Loss of Bbs3 did not affect BBSome subunit protein levels. Shown here are Western blots of total protein lysates from WT and *Bbs3*$^{-/-}$ testes and blotted with antibodies against BBSome subunits. (*B*) Loss of the BBSome did not affect Bbs3 protein level. Shown are Western blots of total protein lysates from WT, *Bbs1*^{M390R}, *Bbs2*$^{-/-}$, *Bbs4*$^{-/-}$, *Bbs6*$^{-/-}$, *Bbs7*$^{-/-}$, and *Bbs3*$^{-/-}$ testes and blotted with antibodies against BBS3. (*C*) Bbs3 is not required for the BBSome formation. Shown are Western blots of testes proteins immunoprecipitated with anti-BBS2 antibody. The existence of other BBSome subunits was detected by anti-individual BBSome subunit antibodies. Equal amount initial protein from testes lysates were used. (*D*) Sucrose gradient analysis of testicular protein lysates confirmed that loss of Bbs3 protein did not affect BBSome formation. (*E*) Loss of BBSome formation in cultured kidney cells from *Bbs3*$^{-/-}$ mice. Shown were cultured kidney cells from WT and *Bbs3*$^{-/-}$ mice infected with adenovirus expressing FLAG tagged BBS2. Infected cells were lysed and expressed proteins were pulled down by anti-FLAG antibody. The existence of endogenous BBSome subunits was detected by Western blot.

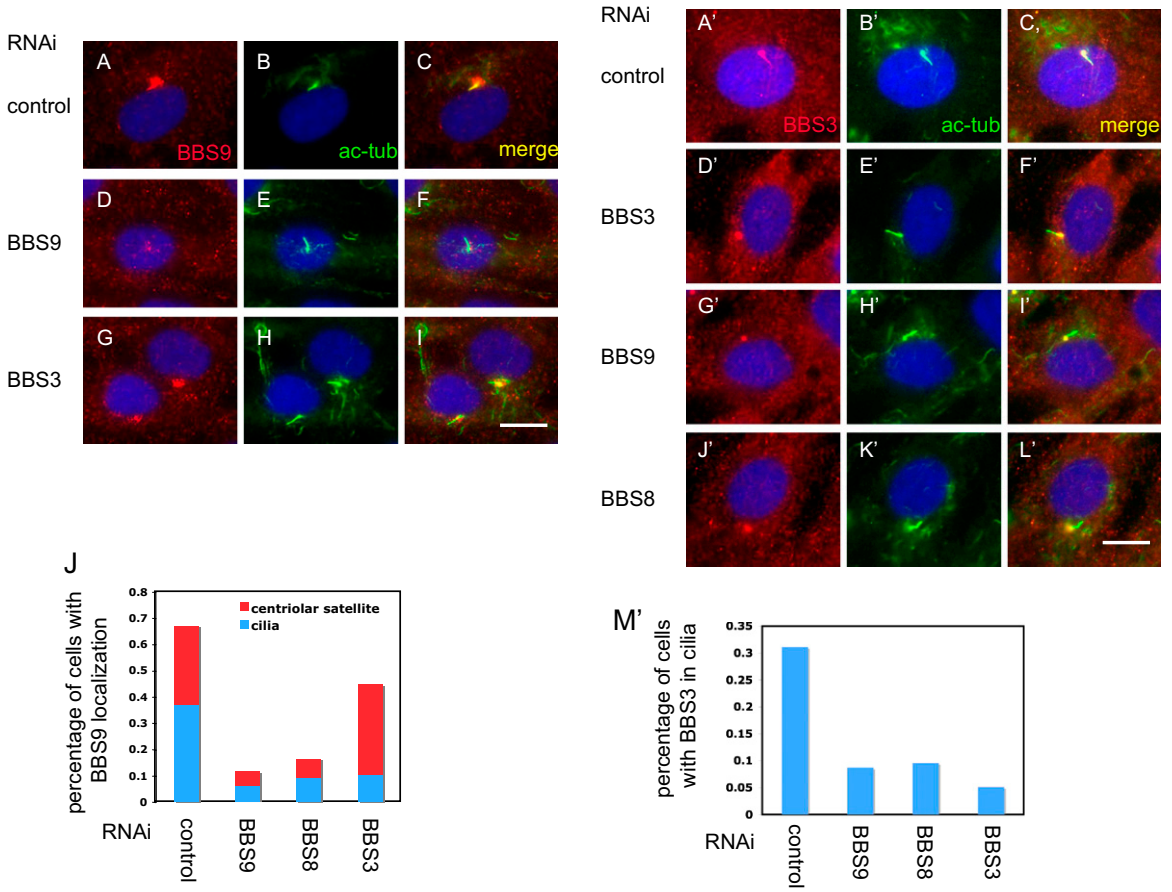

Fig. S4. BBS3 and the BBSome are interdependent for ciliary localization. (*A–J*) The BBSome requires BBS3 for ciliary localization. hTERT-RPE1 cells were depleted of BBS3 protein by RNAi and stained with anti-BBS9 antibody (red) for BBSome localizaton and antiacetylated tubulin antibody (green) for cilia. The BBSome localizes to the cilia and pericentriolar satellites (*A–C*). Staining is demonstrated to be specific as knockdown of BBS9 by RNAi decreases the signal in both regions (*D–F*). Knockdown BBS3 decreases BBS9 signal in the cilia but not signals in the pericentriolar satellites (*G–I*). (*J*) Quantitation of the percentage of cells with BBS9 staining in the cilia and in the pericentriolar satellites. *A′–M′* shows that BBS3 requires the BBSome for ciliary localization. hTERT-RPE1 cells were depleted of BBSome proteins by RNAi and stained with anti-BBS3 antibody (red) and antiacetylated tubulin antibody (green) for cilia. BBS3 localizes to cilia (*A′–C′*). Staining is specific because knockdown of BBS3 by RNAi decreased the signal in cilia; basal body staining is nonspecific because this staining did not decrease with BBS3 knockdown by RNAi (*D′–F′*). BBSome knockdown by RNAi against either BBS9 or BBS8 decreases BBS3 signal in cilia (*G′–L′*). (*M′*) Quantitation of the percentage of cells with BBS3 staining in cilia. Scale bars, 10 μm.

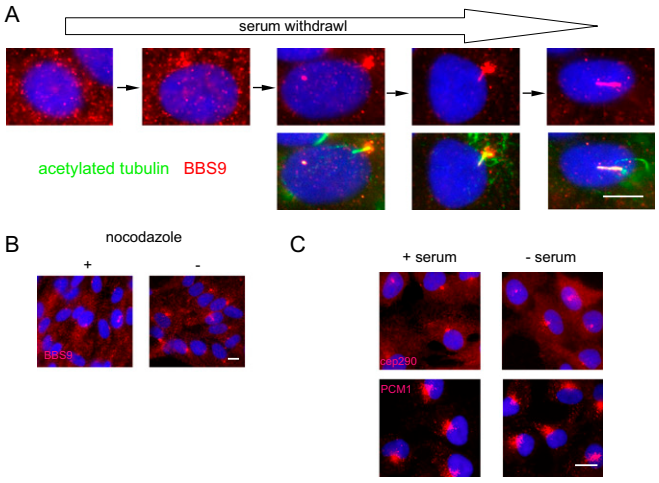

Fig. S5. Dynamic localization changes of the endogenous BBSome inside cells. (*A*) hTERT-RPE1 cells induced to form cilia by serum withdrawal at different time points. BBS9 stain is red and cilia marker acetylated tubulin is green. The dynamic localization changes of the endogenous BBSome depend on intact microtubules. Disruption of microtubules with nocodazole abolishes both pericentriolar satellite and cilia localization of the BBSome (*B*). In contrast, the pericentriolar satellite localizations of cep290 (red) and pericentriolar material 1 (PCM1) (red) are not dependent on serum withdrawal (*C*). Scale bars, 10 μm.

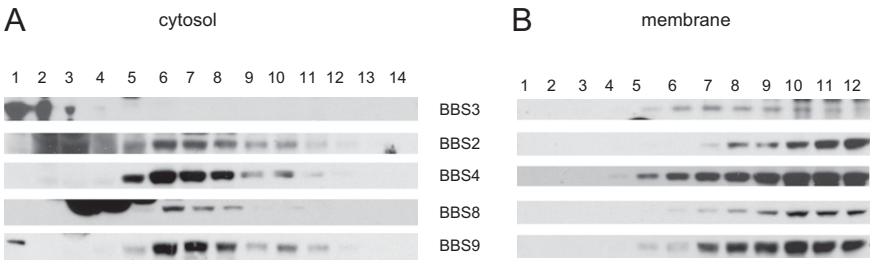

Fig. S6. BBS3 and the BBSome are present in the cytosolic pool and membranes pool. Nonciliated RPE1 (subconfluency with 10% serum) cells were disrupted by mechanic forces and separated into cytosol fractions and membrane fractions. Both fractions were loaded to sucrose gradient. (*A*) Sucrose gradient analysis of cytosol fractions and (*B*) sucrose gradient analysis of membrane fractions.

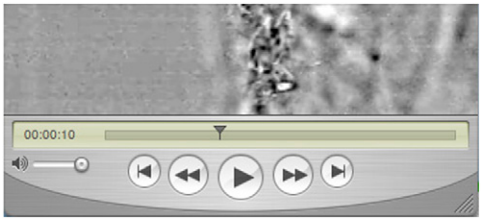

Movie S1. Cilia beating in cultured brain ependymal cells, from *Bbs3*$^{-/-}$ culture. Cultured ependymal cells were transferred to a 37 °C temperature-controlled stage and imaged on a Zeiss LSM 510 META NLO. Ciliated cells were randomly selected and QuickTime movies of ciliary beating were then generated.

Movie S1

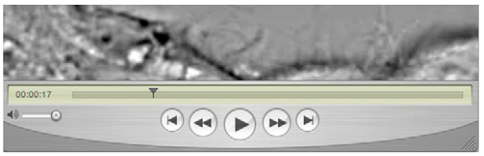

Movie S2. Cilia beating in cultured brain ependymal cells, from WT culture. Cultured ependymal cells were transferred to a 37 °C temperature-controlled stage and imaged on a Zeiss LSM 510 META NLO. Ciliated cells were randomly selected and QuickTime movies of ciliary beating were then generated.

Movie S2